# FINAL REPORT FOR USGS AWARD NUMBER 08HQGR0037

# EVALUATION OF NONLINEAR SITE RESPONSE OF SOFT CLAY USING CENTRIFUGE MODELS

**Principal Investigators:**

Scott J. Brandenberg, Ph.D.
Assistant Professor
Department of Civil and Environmental Engineering
5731 Boelter Hall
University of California, Los Angeles, CA 90095-1593
phone: 310-825-9819; fax: 310-206-2222; email: sjbrandenberg@ucla.edu

Jonathan P. Stewart
Professor
Department of Civil and Environmental Engineering
5731 Boelter Hall
University of California, Los Angeles, CA 90095-1593
phone: 310-206-2990; fax: 310-206-2222; email: jstewart@seas.ucla.edu

**Graduate Student Researchers:**

Kamil B. AfacanDepartment of Civil and Environmental Engineering
University of California, Los Angeles

Alek Harounian
Department of Civil and Environmental Engineering
University of California, Los Angeles

Lijun Deng
Department of Civil and Environmental Engineering
University of California, Davis

Dongsoon Park
Department of Civil and Environmental Engineering
University of California, Davis

Term covered:
July 1, 2008 - September 30, 2010

## TABLE OF CONTENTS

Table of Contents ..... ii

Abstract ..... iii

1 Background and Motivation ..... 1

2 Centrifuge Test Program ..... 3
- 2.1 Model Configuration ..... 4
- 2.2 Soil Properties ..... 8
- 2.3 Base Motion Sequence ..... 11
- 2.4 Data Processing and Archiving ..... 14
- 2.5 Example Data ..... 17

3 Preliminary Observations ..... 25

4 Conclusions ..... 28

5 Acknowledgments ..... 29

6 References ..... 30

Abstract

Research project #08HQGR0037 used two centrifuge models to evaluate nonlinear site response of soft clay. Testing was performed at the NEES@UCDavis centrifuge facility on the 9-m radius large geotechnical centrifuge. The two models were composed of San Francisco Bay mud constructed in lifts separated by thin sand seams. The prototype depth of the centrifuge models was approximately 30m, and the average shear wave velocities (i.e., $V_{s30}$) for the models were 100 and 109 m/s. Suites of ground motions that are scaled versions of motions recorded during past earthquakes were imposed on the base of the models, and the response of the models was recorded by over 50 accelerometers. Additionally, pore pressure transducers and linear potentiometers were utilized. Shear strains of more than 1% were mobilized in the models, which is important for validation of nonlinear site response codes. Although nonlinear site response codes are widely recognized as superior to equivalent linear codes at sites when large shear strains (i.e., >1%) occur, very little data exists at such large strain levels for validating nonlinear codes. All test data collected during this experimental study is archived and will be made publicly available at http://nees.org/warehouse/project/696.

# 1 BACKGROUND AND MOTIVATION

Ground motion prediction equations (GMPE; also known as attenuation relationships) are used in seismic hazard analyses to provide a probabilistic distribution of a particular ground motion intensity measure (*IM*) conditional on source, path, and site parameters. Estimates from such relationships represent averaged values across the range of possible site conditions associated with the GMPE. Site condition is often defined by the average shear wave velocity in the upper 30 m ($V_{s30}$). However, many profiles could produce the same $V_{s30}$ and yet have significantly different site response. To account for site-specific attributes as part of a ground motion evaluation, site response analyses are performed that may focus on sediment response to upwardly propagating body waves (ground response effects), basin effects, and surface topography. The focus of the present work is on the first of these site effects (ground response), which can dominate the site response at low to medium periods for level-ground sites.

There are two general categories of methods for analysis of ground response effects – equivalent-linear (EL) and non-linear (NL) analysis. EL techniques model the soil as visco-elastic, with stiffness and damping properties selected to be compatible with the level of shear strain. The linear assumption allows the solution to be formulated in the frequency domain, with time-domain results produced via an inverse Fourier transform (Kramer, 1996). NL analyses are always performed in the time domain, with shear modulus and damping defined by a plasticity formulation that explicitly models expected soil nonlinearity as a function of shear strain.

Frequency-domain, equivalent-linear methods of performing site response analysis remain significantly more popular in practice than time-domain, nonlinear methods (Kramer and Paulsen, 2004). One reason this practice persists is that parameter selection for frequency-domain analysis is relatively straightforward, requiring only mass density, shear wave velocity,

and nonlinear modulus reduction and damping versus shear strain curves. As a profession, we are well equipped to provide estimates of these quantities on a site-specific basis at reasonable cost.

In contrast, time-domain, nonlinear methods of analysis require the use of parameters that are less familiar to most engineers and/or relatively difficult to obtain. Nonetheless, there is general consensus in the geotechnical engineering community that nonlinear analyses are required for "large strain" conditions (generally taken as shear strain $\gamma > 1\%$). A recent project sought to overcome the hurdles that have limited the practical application of nonlinear ground response analysis methods by (1) establishing protocols for parameter selection, (2) validating the parameter selection protocols against available data from vertical arrays, and (3) identifying conditions where the results of EL and NL analyses are significantly different from each other (Kwok et al. 2007; Kwok et al. 2008). Proper validation of NL methods is difficult due to the scarcity of high quality experimental data available for earthquake ground motions large enough to induce "large strain" conditions. A key finding of the recent research project was the need for more high-quality large amplitude ground motion data from downhole arrays.

There are two potential sources of data for verification of the results of the nonlinear codes using the established usage protocols. The optimal source is vertical arrays because they represent actual ground shaking under realistic conditions. The vertical array data considered by Kwok et al. (from Kiknet, CSMIP arrays, Lotung, etc.) exhibited peak strains that generally ranged from 0.01 to 0.2%. Those strain levels fall below those for which most Geotechnical Engineers would consider running nonlinear analyses. More recently, a downhole array at the Kashiwazaki-Kariwa nuclear power plant recorded strong ground motions during the 2007 Niigata Ken Chuetsu Oki earthquake. This is the first case history known to the PI's where a

downhole array recorded strong enough ground shaking to validate nonlinear site response codes.

The problem of limited large-strain validation data sets was addressed in this research using centrifuge modeling. This was also the concept behind a previous USGS-NEHRP proposal awarded to Elgamal and Kutter, which ultimately resulted in publications by Elgamal et al. (2005), and Lai et al. (2001). Unfortunately, that work did not provide data sets that could be used for the type of model validation described above because the soil container used in the centrifuge likely significantly affected the results, although the degree of influence was unresolved. Moreover, the testing was performed with dense sandy soils, which are not the type of soil for which large-strain ground response effects would normally be anticipated.

## 2 CENTRIFUGE TEST PROGRAM

This research project studied the nonlinear site response behavior of soft clay using two centrifuge model tests performed at the University of California, Davis large centrifuge facility. The first model, AHA01, was tested in May 2009 and the second model, AHA02 was tested in March 2010. The models were constructed from San Francisco bay mud, which is a natural marine clay encountered along the margins of the San Francisco Bay. Bay Mud caused significant ground motion amplification in the 1989 Loma Prieta earthquake, which led to structural damage in Oakland and San Francisco (e.g., Seed et al., 1991).

The centrifuge was spun to 57.2g, and the prototype depth of the models was approximately 30m. The pore fluid was water. The models were heavily instrumented with accelerometers, pore pressure transducers, and linear potentiometers to measure the response of the models to the simulated earthquakes. Each model was shaken by a sequence of realistic ground motions with a

range of intensities (small to large). The models were constructed in a new hinged-plate container that has essentially zero lateral stiffness and is therefore well-suited to site response studies. This container had not been used in previous experiments.

This research project was granted a NEES shared-use designation, which means that management, operations, and maintenance costs associated with the project were funded by the National Science Foundation through the George E. Brown Network for Earthquake Engineering Simulation (NEES). A requirement of NEES projects is that all experimental data is archived and curated in a central repository called NEEShub (www.nees.org). The test data recorded in this study has been made available at:

http://nees.org/warehouse/project/696

As of the date of writing this report (December 2010), much of the data has been uploaded to the repository, but the data has not yet been curated and made public. We anticipate the data will be fully released in early 2011.

### 2.1 Model Configuration

The centrifuge models consisted of soft San Francisco bay mud separated by thin layers of dense sand that served as drainage boundaries. The top lift of clay was overlain by a layer of sand to protect the clay from desiccation due to wind currents during spinning and to provide some mass to drive the underlying clay into the nonlinear range. Figures 1 and 2 show the configuration of the centrifuge models. Approximately 100 sensors were embedded in each model, over half of which were accelerometers used to measure ground motion throughout the model. The models were constructed using a hydraulic press to consolidate the clay in lifts with

final thicknesses of approximately 5 to 6 cm. The clay could not be constructed in a single lift because the time required for consolidation would have been excessive.

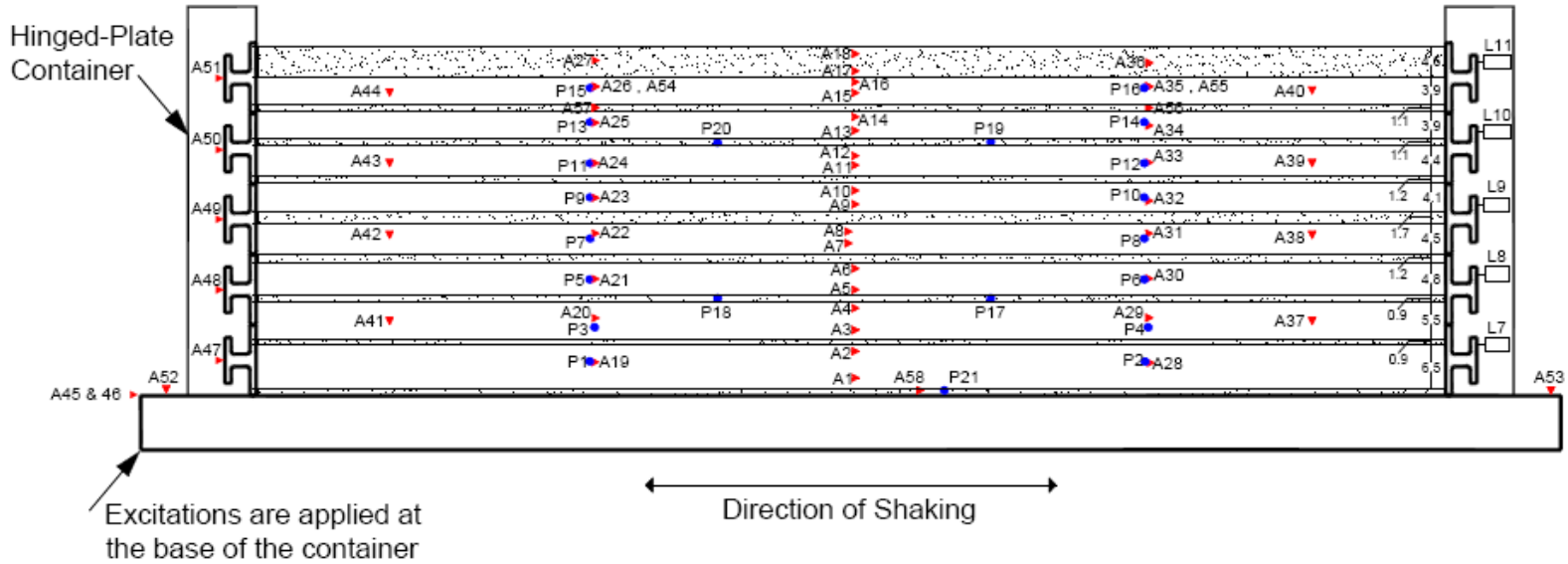


**Figure 1. Configuration of model AHA01.**

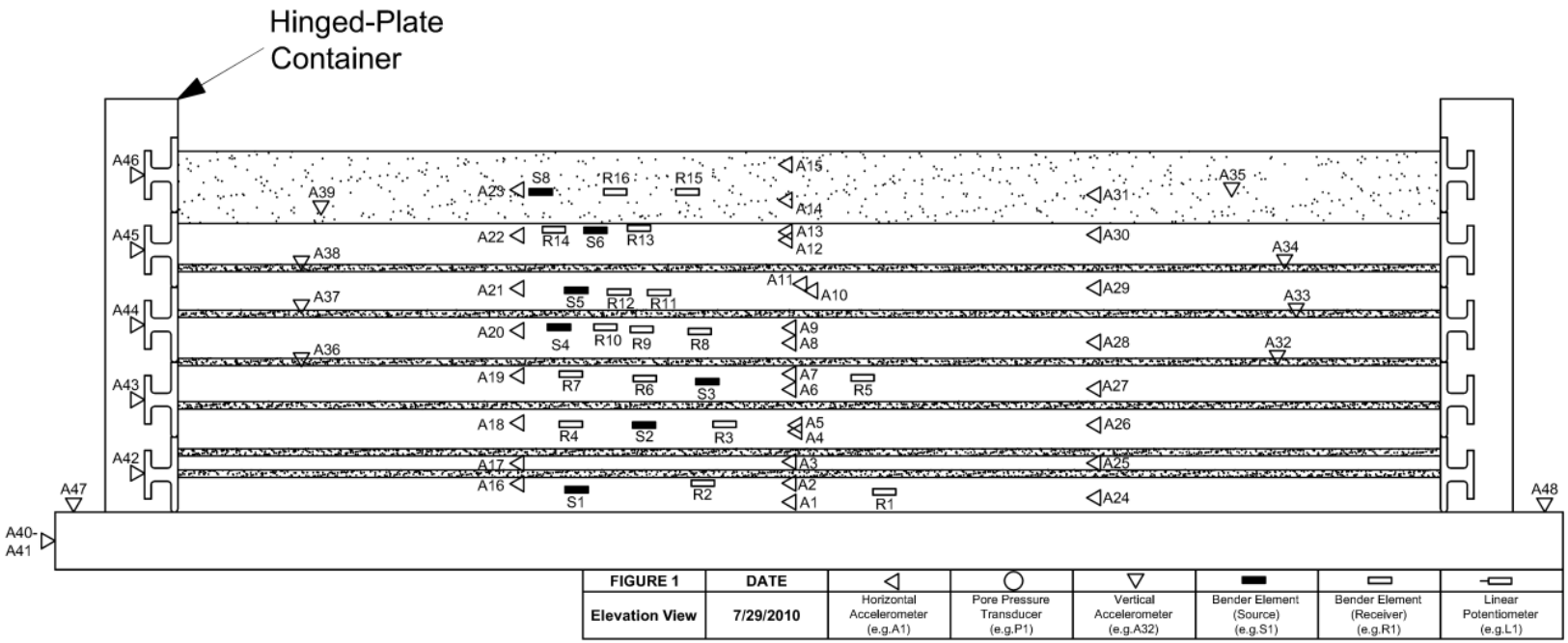


**Figure 2. Configuration of model AHA02.**

**Figure 3. (a) Hinged plate container utilized in this study and (b) shear beam container utilized in previous site response studies.**

The model container utilized in this study was a new flexible hinged-plate container that had never before been utilized on the UC Davis large centrifuge (Fig. 3). Previous site response studies utilized shear beam containers consisting of aluminum rings separated by flexible rubber layers (Fig. 4). Shear beam containers are flexible relative to a stiff soil profiles, and therefore impose boundary conditions that are reasonably consistent with one-dimensional site response. However, as the soil softens, the influence of the container becomes more significant and can result in boundary conditions that are not one-dimensional. For example, sloshing of liquefied sand has been observed in the shear beam containers. The hinged-plate container, on the other hand, consists of plates resting on ball bearings that are free to move in the shaking direction. As a result, the container has essentially zero lateral stiffness resulting in more realistic one-dimensional boundary conditions. Furthermore, the plates on the ends of the container are free to rotate, thereby conforming more naturally to the deformed shape of the soil profile.

## 2.2 Soil Properties

Properties of the soil used in the models are summarized in Table 1. Laboratory tests performed as part of this study included consolidation, specific gravity, Atterberg limits, and

water content. Additionally, undrained shear strength was measured using a small hand vane shear device immediately after spinning down the centrifuge. Results of these laboratory tests are available in the data reports that can be downloaded through NEEShub.

**Table 1. Properties of soil used in the centrifuge models.**

| ***Parameter*** | ***CLAY*** | ***SAND*** |
|---|---|---|
| Soil type | Bay Mud | Nevada Sand |
| USCS | MH | SP |
| Specific gravity | 2.65 | 2.644 |
| Mean grain size, $D_{50}$ (mm) | - | 0.17 |
| Coefficient of uniformity, $C_u$ | - | 1.64 |
| Maximum dry unit weight, $\gamma_{max}$ (kN/m$^3$) | - | 16.9 |
| Minimum dry unit weight, $\gamma_{min}$ (kN/m$^3$) | - | 13.9 |
| Relative density (%) | - | 80 |
| Average total unit weight - $\gamma_{avg.}$ (kN/m$^3$) | 16.0 | 19.8 |
| Permeability (cm/s) | - | $3.2 \times 10^{-3}$ |
| PL (%) | 40-43 | - |
| LL (%) | 84-86 | - |
| Average water content of slurry mud is 115% | | |

Profiles of consolidation stress, overconsolidation ratio, undrained shear strength, and shear wave velocity are shown in Fig. 4. Undrained shear strength values were based on the post-test vane shear results combined with strength normalization concepts (e.g., Ladd 1991) as discussed in the data reports. Shear wave velocity measurements were based on travel times from a combination of bender element test data, and low-amplitude high-frequency sine waves imposed on the base of the model. Additionally, knowledge of the dependence of $V_s$ on consolidation stress was used to develop the profiles in Fig. 4. Details are presented in the data reports.

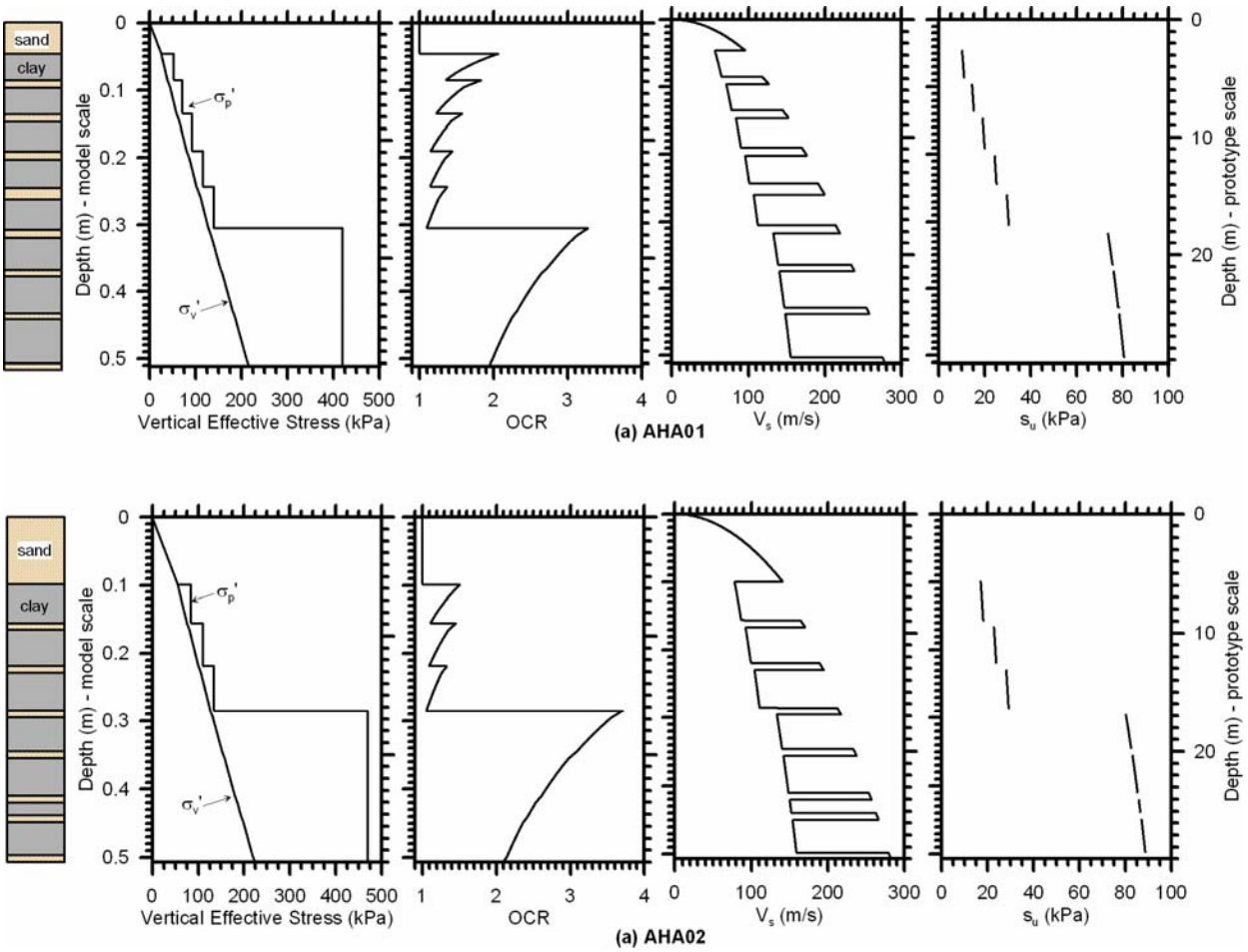


**Figure 4. Profiles of vertical effective stress, overconsolidation ratio, shear wave velocity, and undrained shear strength for (a) model AHA01 and (b) model AHA02.**

During consolidation of the lifts of clay, we recorded pore water pressure near the center of each lift, vertical displacement of the hydraulic press plate, and the applied load (applied load measured in AHA02 only). These data are archived on NEEShub and an example of the time-dependence of settlement and pore pressure is shown in Fig. 5 for the 4th stage for test AHA01. The lifts were consolidated in stages and the vertical pressure was slowly increased as the pore pressure dissipated and undrained shear strength increased. Applying pressure to the clay too

quickly can cause the clay slurry to ooze out of the model container, which necessitated the staged construction procedure.

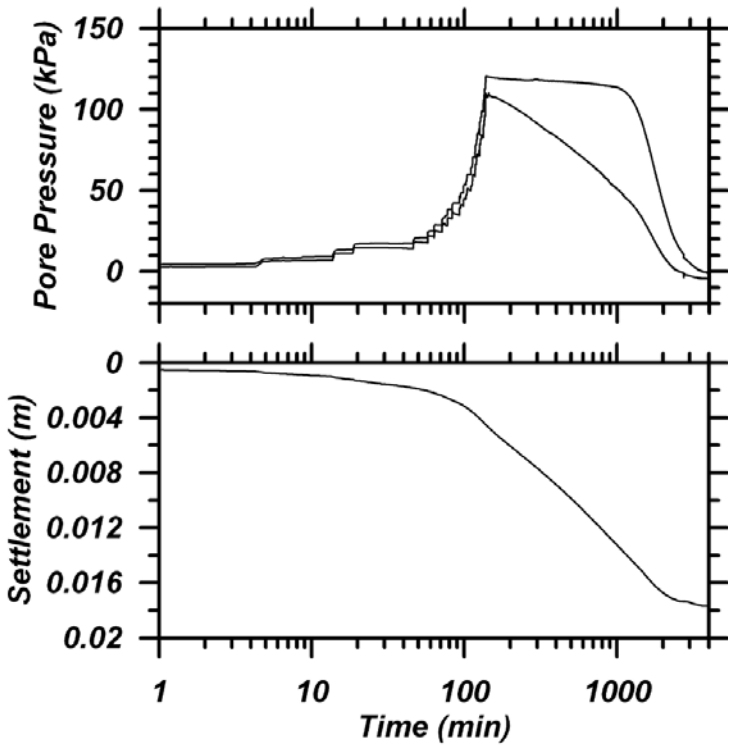


**Figure 5. Consolidation data for 4th stage for model AHA01.**

## 2.3 Base Motion Sequence

A total of 34 shaking events were applied to the base of model AHA01 (23 on May 14th and 11 on May 27th) and 24 motions were applied to the base of model AHA02. The sequence of motion is shown in Tables 2 and 3 for AHA01 and AHA02, respectively.

**Table 2. Ground motion sequence for AHA01.**

| *Event ID* | *Name of Motion* | *Time* | *Date* | *Data File Name* | *Amp Factor* | *PCB Gain* | *Freq. (Hz)* | *CGL* |
|---|---|---|---|---|---|---|---|---|
| *Spin Up* | - | 12:53 | 5/14/2009 | - | - | - | - | - |
| AHA01-S1 | Sine Wave | 17:09 | 5/14/2009 | 05142009@161802@170941@77.5rpm | 0.1 | 10 | 286 | CGL_2 |
| AHA01-S2 | Sine Wave | 17:56 | 5/14/2009 | 05142009@175349@175655@77.4rpm | 0.3 | 10 | 286 | CGL_2 |
| AHA01-S3 | Sine Wave | 18:11 | 5/14/2009 | 05142009@175349@181208@77.3rpm | 1 | 10 | 286 | CGL_2 |
| AHA01-S4 | CYC160_Command4.prn | 19:36 | 5/14/2009 | 05142009@175349@193534@77.4rpm | 0.3 | 10 | - | CGL_2 |
| AHA01-S5 | CYC160_Command4.prn | 19:44 | 5/14/2009 | 05142009@175349@194507@77.3rpm | 1 | 10 | - | CGL_2 |
| AHA01-S6 | HEC000_Command4.prn | 20:08 | 5/14/2009 | 05142009@175349@200853@77.5rpm | 0.9 | 10 | - | CGL_2 |
| AHA01-S7 | HEC000_Command4.prn | 20:16 | 5/14/2009 | 05142009@175349@201622@77.7rpm | 3.5 | 10 | - | CGL_2 |
| AHA01-S8 | HEC000_Command4.prn | 20:32 | 5/14/2009 | 05142009@175349@203230@77.5rpm | 2 | 10 | - | CGL_2 |
| AHA01-S9 | NIS000_Command4.prn | 20:49 | 5/14/2009 | 05142009@204756@204916@77.4rpm | 0.3 | 10 | - | CGL_2 |
| AHA01-S10 | NIS000_Command4.prn | 21:06 | 5/14/2009 | 05142009@204756@210623@77.3rpm | 0.9 | 10 | - | CGL_2 |
| AHA01-S11 | TCU045_N_Command4.prn | 21:32 | 5/14/2009 | 05142009@204756@213331@77.4rpm | 0.5 | 10 | - | CGL_2 |
| AHA01-S12 | TCU045_N_Command4.prn | 21:40 | 5/14/2009 | 05142009@204756@214054@77.7rpm | 1 | 10 | - | CGL_2 |
| AHA01-S15 | CYC160_Command4.prn | 22:00 | 5/14/2009 | 05142009@215809@220241@77.8rpm | 10 | 1 | - | CGL_1 |
| AHA01-S16 | CYC160_Command4.prn | 22:15 | 5/14/2009 | 05142009@215809@221735@77.8rpm | 5.5 | 1 | - | CGL_1 |
| AHA01-S17 | HEC000_Command4.prn | 22:25 | 5/14/2009 | 05142009@215809@222533@77.4rpm | 6 | 1 | - | CGL_1 |
| AHA01-S18 | HEC000_Command4.prn | 22:30 | 5/14/2009 | 05142009@215809@223235@77.9rpm | 12 | 1 | - | CGL_1 |
| AHA01-S19 | NIS000_Command4.prn | 22:40 | 5/14/2009 | 05142009@215809@224134@77.9rpm | 5 | 1 | - | CGL_1 |
| AHA01-S20 | TCU045_N_Command4.prn | 22:52 | 5/14/2009 | 05142009@215809@225228@77.8rpm | 5 | 1 | - | CGL_1 |
| AHA01-S21 | NIS000_Command5.prn | 23:01 | 5/14/2009 | 05142009@215809@230139@77.7rpm | 5 | 1 | - | CGL_1 |
| AHA01-S22 | NIS000_Command5.prn | 23:10 | 5/14/2009 | 05142009@215809@231021@77.6rpm | 13 | 1 | - | CGL_1 |
| AHA01-S23 | TCU045_N_Command5.prn | 23:24 | 5/14/2009 | 05142009@215809@232409@77.9rpm | 5 | 1 | - | CGL_1 |
| AHA01-S24 | TCU045_N_Command5.prn | 23:32 | 5/14/2009 | 05142009@215809@233205@77.6rpm | 13 | 1 | - | CGL_1 |
| AHA01-S25 | SCS052_123_it3.shk | 23:55 | 5/14/2009 | 05142009@215809@235507@77.7rpm | 1 | 1 | - | CGL_1 |
| *Spin Down* | - | 0:10 | 5/15/2009 | - | - | - | - | - |
| *Spin Up* | - | 11:08 | 5/27/2009 | - | - | - | - | - |
| AHA01-S27 | Sine Wave | 16:30 | 5/27/2009 | 05272009@150800@162947@77.0rpm | - | 10 | 500 | CGL_5 |
| AHA01-S28 | TCU045_N_Command5.prn | 16:42 | 5/27/2009 | 05272009@164035@164505@77.6rpm | 5 | 1 | - | CGL_3 |
| AHA01-S29 | PRI090_it3.shk | 16:58 | 5/27/2009 | 05272009@164035@165846@77.3rpm | 1 | 1 | - | CGL_3 |
| AHA01-S31 | Sine Wave | 17:12 | 5/27/2009 | 05272009@170858@171230@77.3rpm | - | 10 | 500 | CGL_5 |
| AHA01-S32 | RRS228_it3.shk | 17:19 | 5/27/2009 | 05272009@171609@171944@77.2rpm | 1 | 1 | - | CGL_3 |
| AHA01-S34 | Sine Wave | 17:30 | 5/27/2009 | 05272009@172914@172954@76.9rpm | - | 10 | 500 | CGL_5 |
| AHA01-S35 | WPI046_it3.shk | 17:32 | 5/27/2009 | 05272009@173018@173255@77.0rpm | 1 | 1 | - | CGL_3 |
| AHA01-S37 | Sine Wave | 17:42 | 5/27/2009 | 05272009@173803@174239@77.9rpm | - | 10 | 500 | CGL_5 |
| AHA01-S38 | LGPC090_it3.shk | 17:45 | 5/27/2009 | 05272009@174352@174750@77.6rpm | 1 | 1 | - | CGL_3 |
| AHA01-S39 | SineSweep.shk | 18:06 | 5/27/2009 | 05272009@174352@180440@77.3rpm | 1 | 1 | - | CGL_3 |
| AHA01-S40 | SineSweep.shk | 18:11 | 5/27/2009 | 05272009@174352@181144@77.4rpm | 5 | 1 | - | CGL_3 |
| *Spin Down* | - | 18:28 | 5/27/2009 | - | - | - | - | - |

**Table 3. Ground motion sequence for AHA02.**

| Event ID | Name of Motion | Time | Date | Shake Data | Amp | PCB Gain | Freq. (Hz) | CGL |
|---|---|---|---|---|---|---|---|---|
| Spin Up | - | 5:30 | 3/18/2010 | - | - | - | - | - |
| Consolidation | - | 5:30 - 12:30 | 3/18/2010 | - | - | - | - | - |
| AHA02-S1 | Step | 12:35 | 3/18/2010 | 03182010@053538@123550@78.3rpm | 0.7 | 10 | - | CGL_1 |
| AHA02-S2 | Sine Wave | 12:55 | 3/18/2010 | 03182010@053538@125549@78.3rpm | 0.3 | 10 | 500 | CGL_1 |
| AHA02-S3 | SineSweep.shk | 1:10 | 3/18/2010 | 03182010@053538@130923@78.2rpm | 1 | 10 | - | CGL_1 |
| AHA02-S4 | SineSweep.shk | 1:30 | 3/18/2010 | 03182010@053538@132837@78.2rpm | 5 | 10 | - | CGL_1 |
| AHA02-S5 | NIS000_Command5.prn | 2:10 | 3/18/2010 | 03182010@053538@141104@78.1rpm | 1 | 10 | - | CGL_1 |
| AHA02-S6 | SCS052_123_it3.shk | 14:30 | 3/18/2010 | 03182010@053538@143130@78.3rpm | 0.1 | 10 | - | CGL_1 |
| AHA02-S7 | PRI090_it3.shk | 14:47 | 3/18/2010 | 03182010@053538@144701@78.2rpm | 0.1 | 1 | - | CGL_0 |
| AHA02-S8 | RRS228_it3.shk | 3:09 | 3/18/2010 | 03182010@053538@150852@78.4rpm | 0.1 | 1 | - | CGL_0 |
| AHA02-S9 | WPI046_it3.shk | 3:19 | 3/18/2010 | 03182010@053538@152017@78.4rpm | 0.1 | 1 | - | CGL_0 |
| AHA02-S10 | LGPC090_it3.shk | 3:29 | 3/18/2010 | 03182010@053538@152936@77.8rpm | 0.1 | 1 | - | CGL_0 |
| AHA02-S11 | NIS000_Command5.prn | 3:39 | 3/18/2010 | 03182010@053538@153857@77.6rpm | 6 | 1 | - | CGL_0 |
| AHA02-S12 | SCS052_123_it3.shk | 3:47 | 3/18/2010 | 03182010@053538@154946@77.2rpm | 0.5 | 1 | - | CGL_0 |
| AHA02-S13 | PRI090_it3.shk | 4:05 | 3/18/2010 | 03182010@053538@160510@77.3rpm | 0.3 | 1 | - | CGL_0 |
| AHA02-S14 | RRS228_it3.shk | 4:12 | 3/18/2010 | 03182010@053538@161240@77.6rpm | 0.3 | 1 | - | CGL_0 |
| AHA02-S15 | WPI046_it3.shk | 4:18 | 3/18/2010 | 03182010@053538@161845@77.7rpm | 0.3 | 1 | - | CGL_0 |
| AHA02-S16 | LGPC090_it3.shk | 4:24 | 3/18/2010 | 03182010@053538@162600@77.2rpm | 0.3 | 1 | - | CGL_0 |
| AHA02-S17 | NIS000_Command5.prn | 4:34 | 3/18/2010 | 03182010@053538@163403@77.5rpm | 13 | 1 | - | CGL_0 |
| AHA02-S18 | SCS052_123_it3.shk | 4:51 | 3/18/2010 | 03182010@053538@165115@77.7rpm | 1 | 1 | - | CGL_0 |
| AHA02-S19 | PRI090_it3.shk | 5:31 | 3/18/2010 | 03182010@053538@173148@77.9rpm | 1 | 1 | - | CGL_0 |
| AHA02-S20 | RRS228_it3.shk | 5:53 | 3/18/2010 | 03182010@053538@175314@77.6rpm | 1 | 1 | - | CGL_0 |
| AHA02-S21 | WPI046_it3.shk | 6:08 | 3/18/2010 | 03182010@053538@180808@77.8rpm | 1 | 1 | - | CGL_0 |
| AHA02-S22 | LGPC090_it3.shk | 6:20 | 3/18/2010 | 03182010@053538@182151@77.9rpm | 1 | 1 | - | CGL_0 |
| AHA02-S23 | Sine Wave | 6:32 | 3/18/2010 | 03182010@053538@183434@77.5rpm | 0.3 | 10 | - | CGL_1 |
| AHA02-S24 | Kobe0807.shk | 6:40 | 3/18/2010 | 03182010@053538@184308@77.5rpm | 7 | 1 | - | CGL_0 |
| Spin Down | - | | 3/18/2010 | - | - | - | - | - |

Most of the ground motions used in this study were scaled versions of earthquake recordings. The earthquake, recording station, magnitude, distance, $V_{s30}$, PGA, PGV and PGD for each recording are listed in Table 4. Site conditions for the recorded motions range from soft soil ($V_{s30}$ = 198m/s for the Port Island Kobe motion) to rock ($V_{s30}$ = 705m/s for the Chi-Chi motion). We originally intended to utilize rock motions as inputs to the base of the model container to represent a condition commonly utilized in ground response analysis in which waves are propagated upward from a rock halfspace. This configuration made sense because the bottom of the model container constitutes a relatively stiff base condition. However, we found that these motions did not induce large enough shear strains in the soil (i.e., $\gamma > 1\%$) to fully validate

nonlinear site response codes, in part because the shake table has limited capacity to reproduce high-frequency energy content characteristic of rock motions. Hence, we also utilized motions recorded on softer soil sites that were calibrated for use on the UC Davis centrifuge by Mason et al. (2010). In addition to scaled versions of recorded ground motions, sine waves and sine sweeps were also used. The high-frequency sine waves were utilized to measure travel times between adjacent accelerometers for the purpose of determining shear wave velocity. The sine sweep was utilized to define a small-strain transfer function between the base of the model container and the ground surface.

**Table 4. Characteristics of recorded earthquake ground motions adapted in this study.**

| Motion | Earthquake | Station | $M_w$ | $R_{jb}$ (km) | $V_{s30}$ (m/s) | PGA (g) | PGV (cm/s) | PGD (cm) |
|---|---|---|---|---|---|---|---|---|
| CYC160 | 1979 Coyote Lake | Coyote Lake Dam (SW abutment) | 5.7 | 5.3 | 597 | 0.218 | 15.09 | 1.84 |
| HEC000 | 1999 Hector Mine | Hector | 7.1 | 10.4 | 685 | 0.306 | 34.21 | 17.71 |
| NIS000 | 1995 Kobe | Nishi-Akashi | 6.9 | 7.1 | 609 | 0.486 | 35.73 | 10.75 |
| TCU045 | 1999 Chi Chi | TCU045 | 7.6 | 26 | 705 | 0.473 | 38.89 | 25.52 |
| PRI090 | 1995 Kobe | Port Island (0m) | 6.9 | 3.31 | 198 | 0.278 | 54.20 | 24.72 |
| RRS228 | 1994 Northridge | Rinaldi Receiving Station | 6.7 | 0 | 282 | 0.634 | 109.24 | 28.26 |
| WPI046 | 1994 Northridge | Newhall W Pico Canyon. Rd. | 6.7 | 2.11 | 286 | 0.385 | 79.07 | 30.21 |
| LGPC090 | 1989 Loma Prieta | LGPC | 6.9 | 0 | 478 | 0.784 | 77.15 | 42.67 |

## 2.4 Data Processing and Archiving

All data in this report is presented in prototype scale, unless otherwise stated. Scale factors used to convert the test data from model scale to prototype scale are provided in Table 5. Details of centrifuge scaling laws can be found in Kutter (1994).

**Table 5. Scale factors used to convert the model data to prototype units.**

| Quantity | Prototype Dimension / Model Dimension |
|---|---|
| Time | 57.2/1 |
| Displacement, Length | 57.2/1 |
| Acceleration | 1/57.2 |
| Force | $(57.2)^2/1$ |
| Pressure, Stress | 1/1 |
| Permeability | 57.2/1 |

For the shaking events, data were collected at a sampling rate of 4096 Hz for approximately 10 seconds, and the raw data files were saved as bit counts in binary format. The raw data files were converted to prototype units in ASCII format using a Lab View program. The raw, unprocessed data and the processed data can be found on the NEES project website. The steps used to process the data are:

1. Removal of pre- and post-shake data
2. Sorting
3. Offset
4. Calibration

The details of each procedure are discussed below.

1. <u>Removal of pre- and post-shake data</u>

Approximately 10 seconds of data were recorded for each shaking event (model scale time), but only about 1 second of the data contained the imposed ground motion. Some of the pre- and post-shake data were removed from the records to reduce file size.

2. Sorting

The columns in the raw data files are arranged in an order that corresponds to the amplifier channel numbers rather than the sensor ID's. The data were sorted first by instrument type and sub-sorted by instrument number to facilitate interpretation.

3. Offsets

Offsets were required because voltage zero does not in general correspond with physical zero. For acceleration records, the mean value of each record was subtracted from the entire record. For displacement records, the average of 500 data points of the displacement before the first shake was subtracted from all of the displacement records. Hence, displacements are referenced to the initial undeformed model geometry immediately prior to the first ground motion. For pore pressure transducers, the offset was applied such that zero pressure corresponds to zero gauge pressure (i.e., zero relative to local atmospheric pressure).

4. Calibration

Calibration factors were applied to convert from bits to prototype units. Pore pressure transducers and linear potentiometers were calibrated before the test, and the manufacturer-specified calibration factors were used for the accelerometers. Calibration factors are included in the data reports on the NEEShub website.

A screenshot of the project site from the NEEShub data repository is shown in Fig. 6.

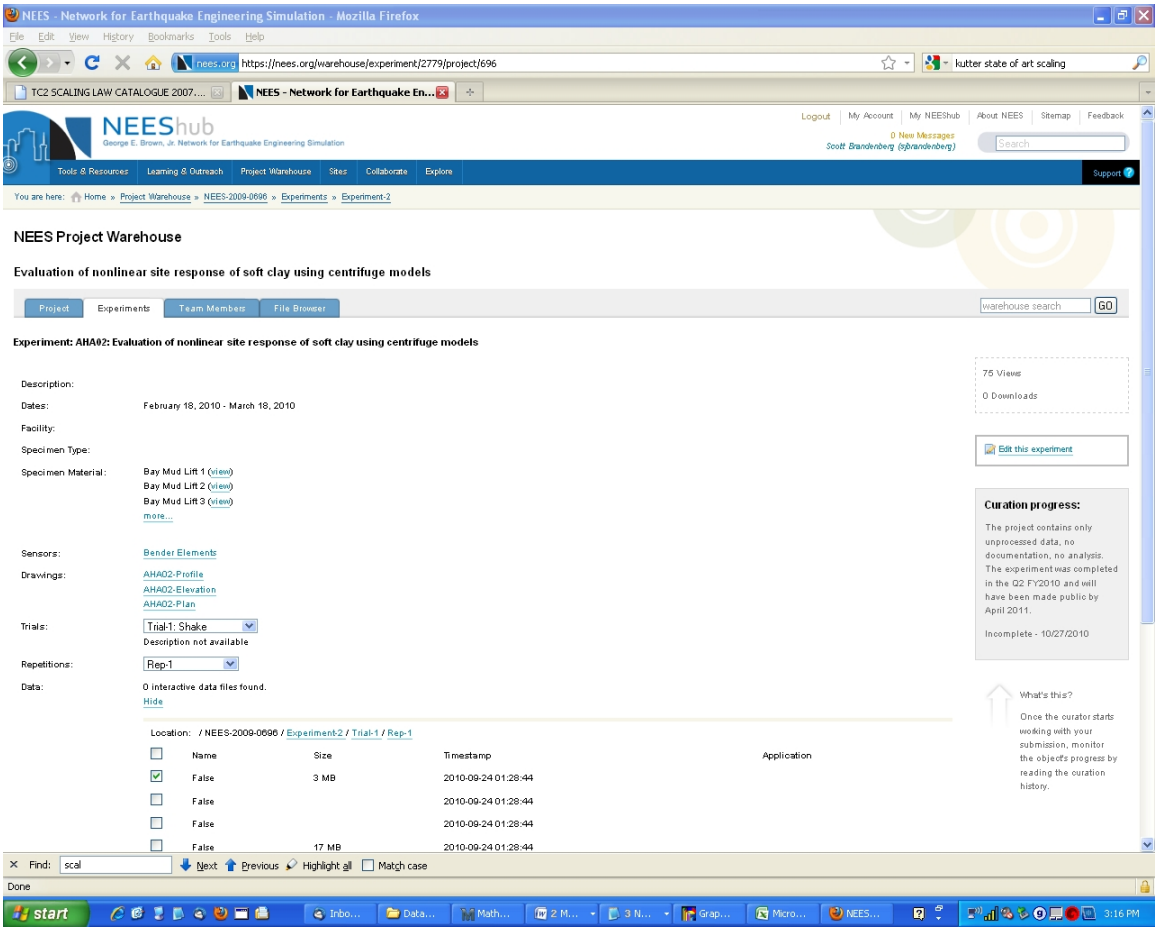


**Figure 6. Screen capture of NEEShub repository (http://nees.org/warehouse/experiment/2779/project0696).**

## 2.5 Example Data

Example data from one of the large ground motions (AHA01-S38) are presented in this section. The data reports on NEEShub contain plots of all of the data quantities recorded for each ground motion. These plots occupy hundreds of pages, and are omitted from this report for brevity. Accelerations and displacements of the five hinged plates of the model container are presented in Figs. 7 and 8, respectively. The displacement at the top ring of the container is approximately 0.3m larger than at the bottom ring over a vertical distance of approximately 30m. This indicates an average peak shear strain of 1% was induced over the height of the container,

though more shear strain was observed near the top of the container than at the bottom. This observation indicates that large shear strain amplitudes were mobilized in the models; it is these large strain amplitudes that are of interest for validation of nonlinear ground response analysis codes.

Fig. 9 shows pore pressure records obtained during the large shaking event. The records show that very little pore pressure was generated despite the large shear strains mobilized in the clay. The primary purpose of the pore pressure transducers was to monitor consolidation during spin up, and any permanent pore pressures induced by shear strains in the clay during shaking. Transient pore pressure changes are more difficult to measure because a small amount of water must flow out of the soil into the transducer in order to record pressure, and this flow may not be possible due to the low permeability of the clay. Hence, it is unclear the extent to which the transient pore pressure response shown in Fig. 9 is representative of the actual clay behavior.

Horizontal variations of recorded accelerations across one lift of the model are presented in Fig. 10. The peak acceleration values recorded on the ring of the container and at three positions within the soil mass at the same elevation have very similar amplitudes. The motion on the ring of the container recorded by sensor A50 had a bit more content at high frequency (i.e., above 20 Hz), and at lower frequency (i.e. below 0.1Hz) as shown in the Fourier amplitude spectra in Fig. 11. Furthermore the peak of the spectrum is slightly higher (i.e., in the frequency band from 0.2 to 0.5Hz), which may be attributed to the slightly higher elevation of A50 relative to the other three sensors. In general, the four motions are very similar in the frequency band from 0.1Hz to 10Hz, which is an indication that the container performed well in the frequency band of interest. Future work will be required to determine the extent to which the good container performance compares with past centrifuge studies that utilized shear beam containers.

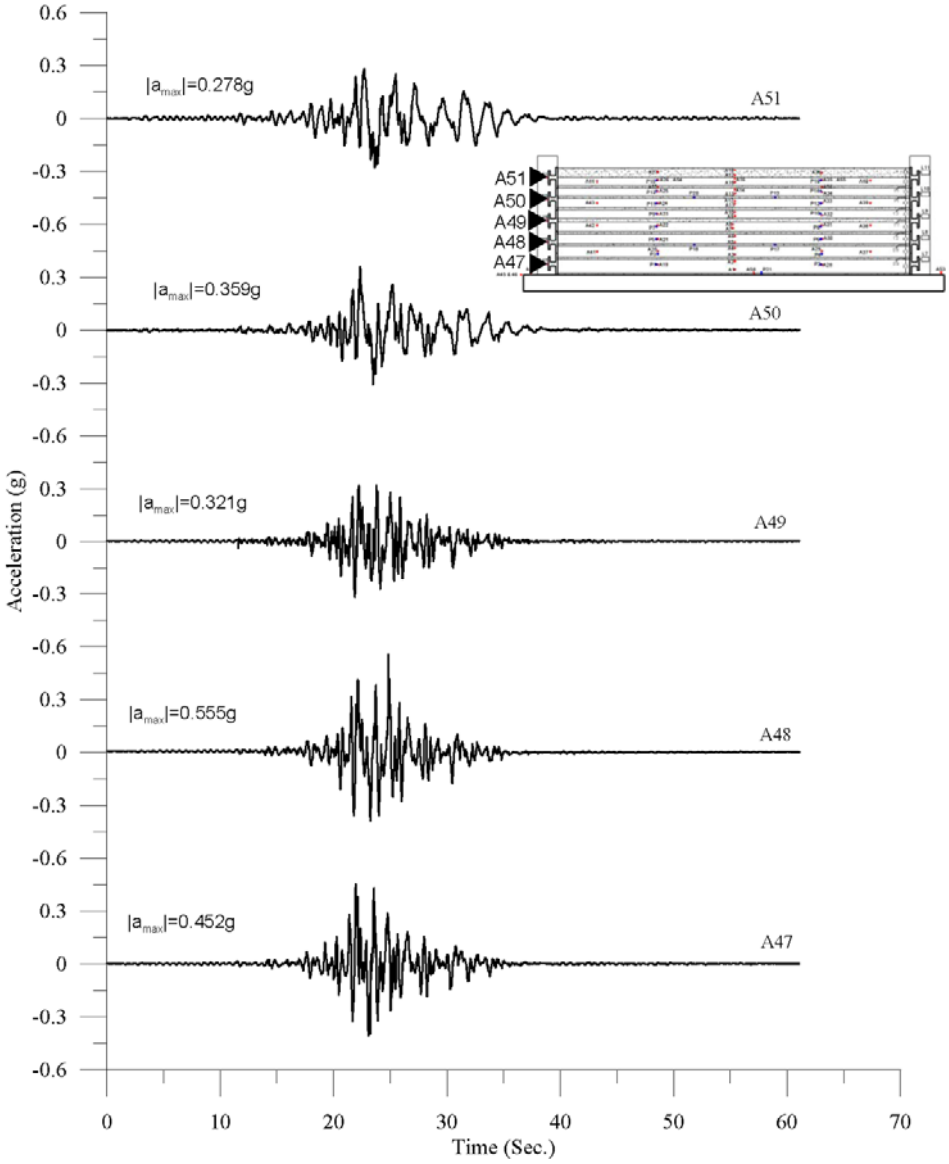


**Figure 7. Acceleration records for rings of model container.**

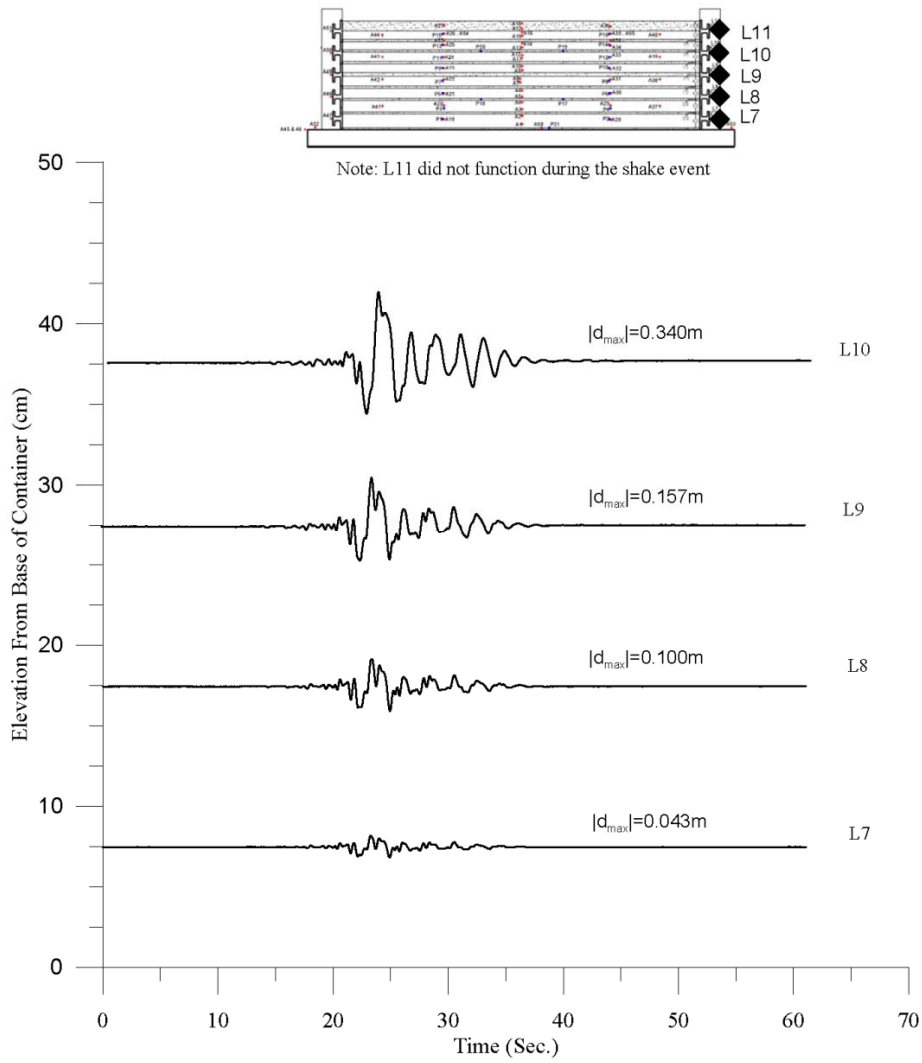


**Figure 8. Displacement records for rings of model container.**

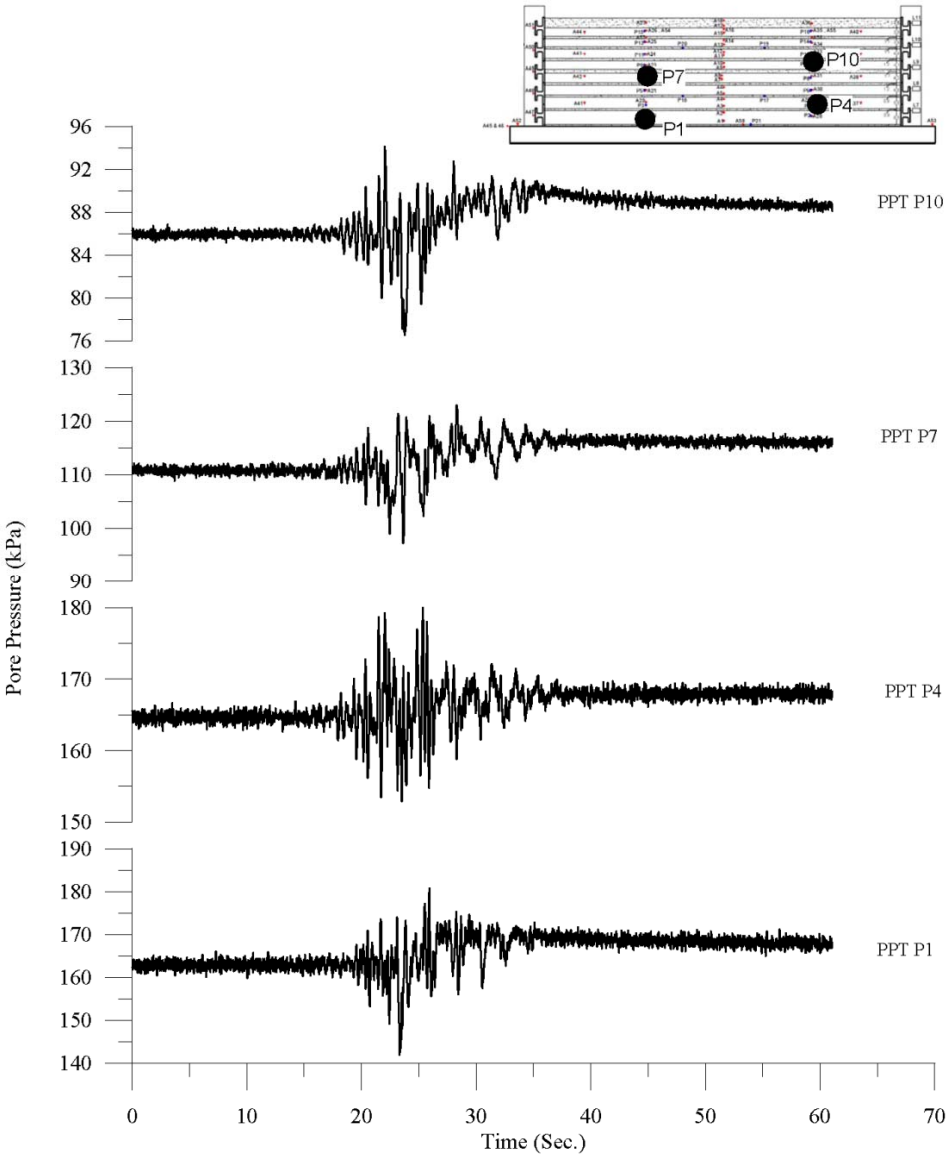


**Figure 9. Selected pore pressure records.**

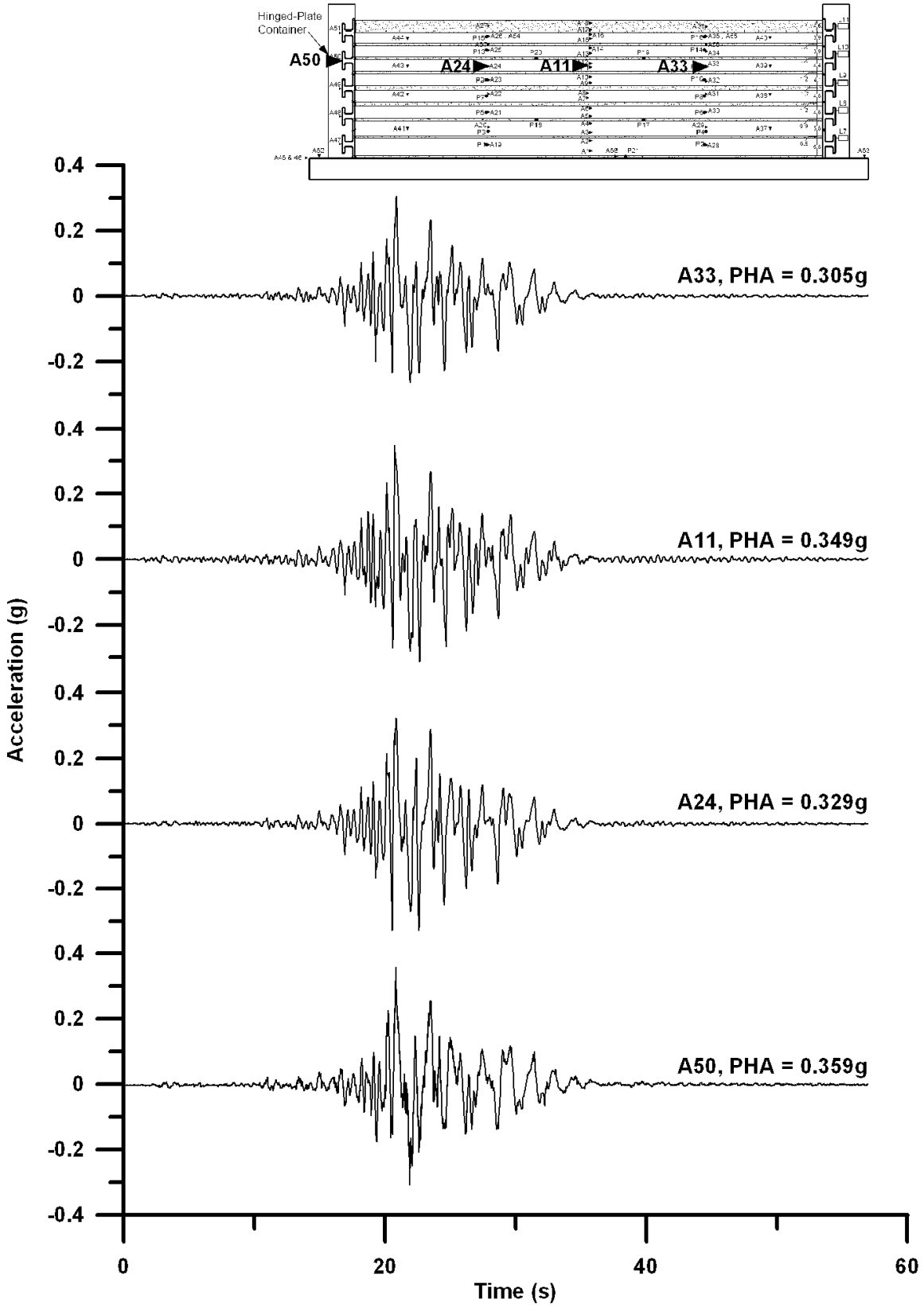


**Figure 10. Horizontal acceleration and displacement records for lift 6 showing horizontal variation of ground motion.**

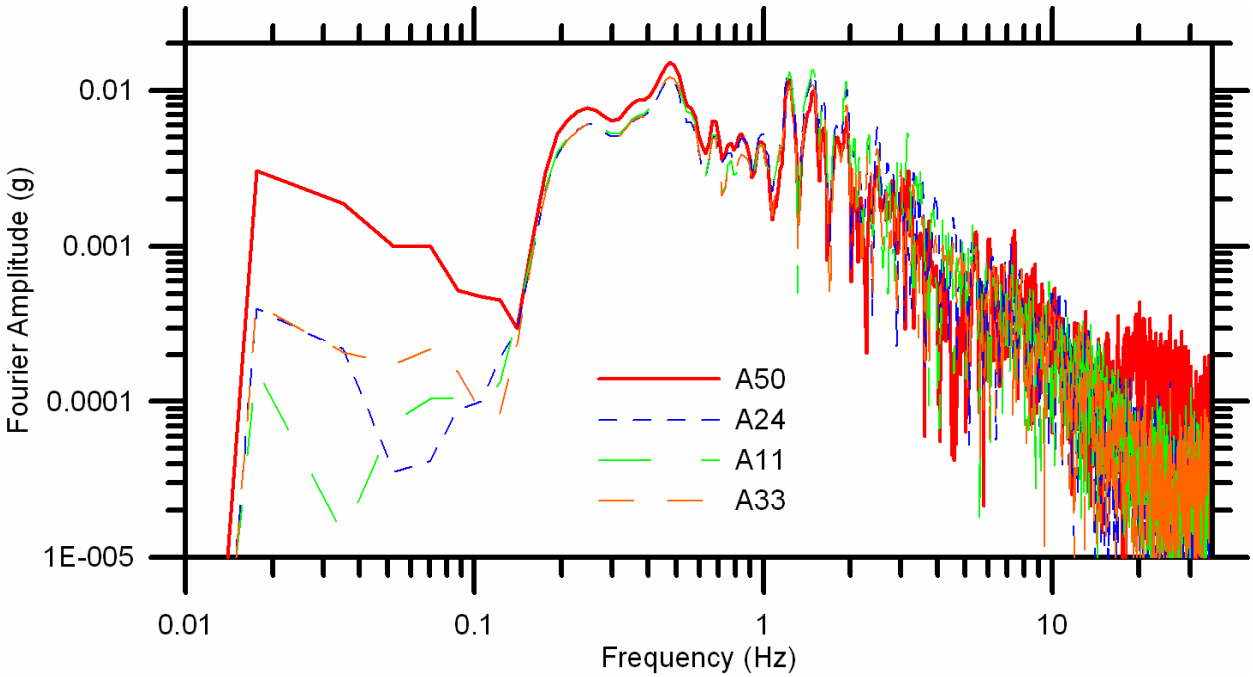

**Figure 11. Fourier amplitude spectra for motions in Fig. 10.**

Fig. 12 shows vertical accelerations recorded at the base of the model container. Rocking of the container often occurs as a result of the flexibility in the elastomeric bearings on which the centrifuge model container rests. Rocking was present in this test, as shown by the out-of-phase vertical accelerations recorded on the north and south end of the model container. Additional effort will be required to quantify the influence of container rocking on the recorded site response behavior.

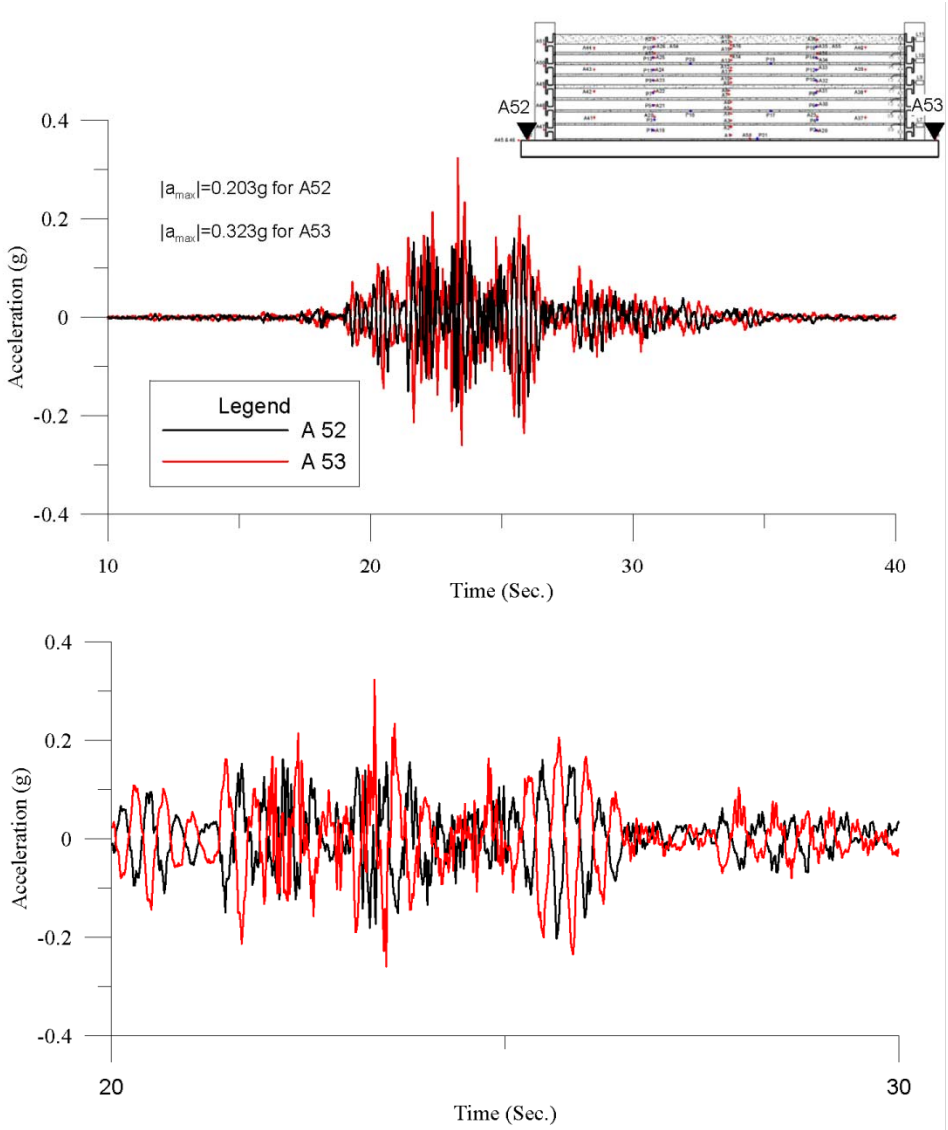


**Figure 12. Acceleration records from base accelerometers on the north and south ends of the model container**

## 3 Preliminary Observations

Our efforts have been devoted nearly entirely to conducting the tests and archiving the experimental data, and firm conclusions have not yet been made from the experimental data. Nevertheless, some basic analysis is presented in this section to demonstrate the value of the data obtained during these experiments. Fig. 13 presents 5% damped linear elastic acceleration response spectra at the base and at the surface for test AHA01, which utilized the Chi-Chi ground motion scaled to PHA=0.012g, 0.035g, 0.142g, and 0.344g.

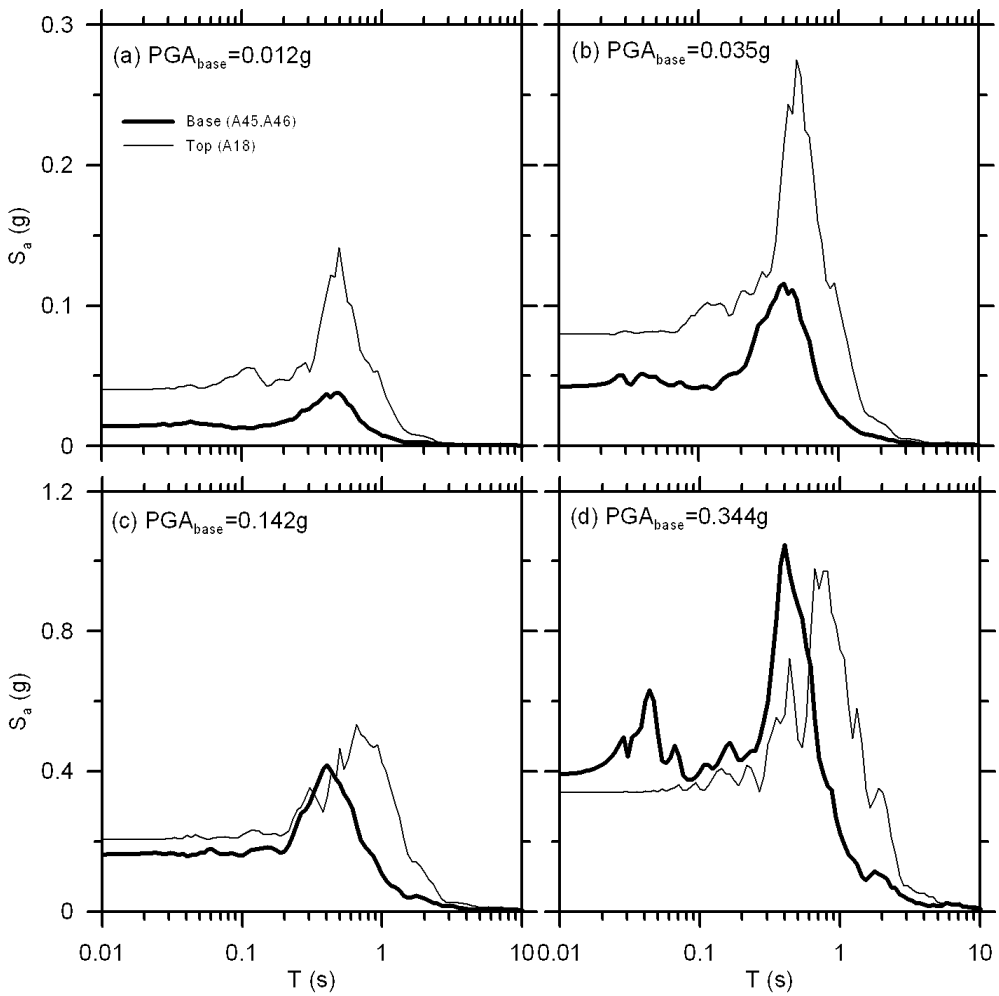


**Figure 13. Acceleration response spectra for base and top of model AHA01 for the Chi-Chi ground motion.**

The following observations from Fig. 13 indicate that the soil column experienced nonlinear response:

(i) at short periods, the response spectrum at the surface is significantly higher than the response spectrum at the base for the smallest motion, and the spectral accelerations become closer together as shaking intensity increases. This reduction in short-period amplification is caused by the increase in damping in the soil as significant shear strains are mobilized.

(ii) the spectral period at which the largest amplification occurs (which is the first mode site period) shifts from approximately 0.95 sec for weak shaking to 1.3 sec for the strongest shaking. This shift is caused by a reduction in the shear modulus of the soil at large shaking amplitude and the corresponding increase in natural period of the model.

The nonlinear effects are more clearly observed in the ratios of response spectra at the surface and the base, as shown in Fig. 14. Short-period amplification decreases as ground motion intensity increases, which is a clear indication of nonlinear soil response. The site period corresponds to the peak of this ratio (0.95-1.3 sec). Long-period amplification is independent of shaking intensity. Hence, the ground motion is amplified at long period, but the phenomenon is essentially linear and therefore independent of PHA.

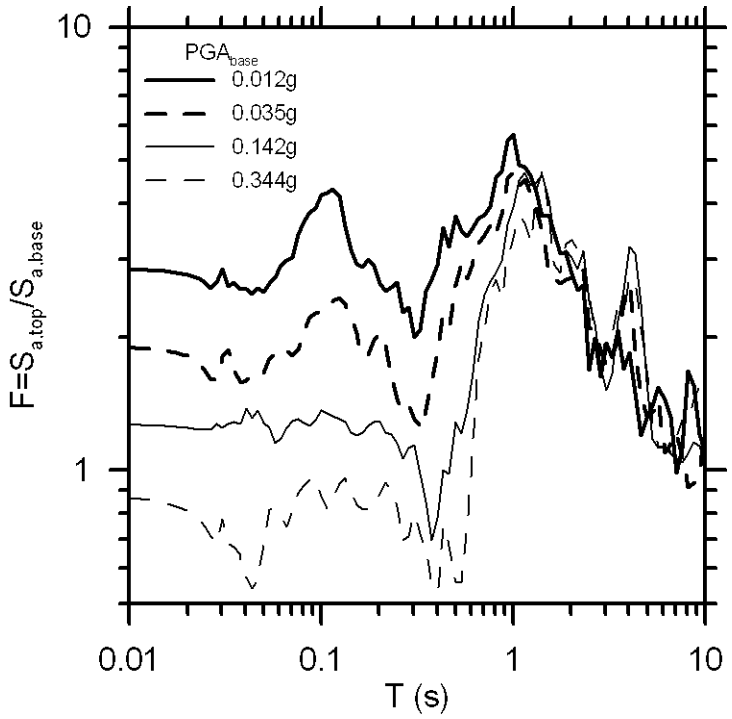


**Figure 14. Spectral acceleration amplification factor for model AHA01 for the Chi-Chi ground motion.**

Response spectral amplification factors (surface/base) were computed for all of the motions utilized in tests AHA01 and AHA02. Fig. 15 shows amplification factors at periods of 0.01, 0.1, and 1.0 s plotted versus peak horizontal acceleration imposed on the base of the model. Also included on the figure are empirical amplification factors from the Boore and Atkinson (2008) ground motion prediction equation (GMPE). The comparison with the GMPE is not an apples-to-apples comparison because the data are comparing spectral acceleration ratios between the ground surface and base of the model container (i.e., surface to within motion for a single site), whereas the GMPE's represent the ratio of spectral acceleration on the surface of a site on soft soil relative to the surface of a site at a reference $V_{s30}$ (i.e., surface to surface for two different sites). Furthermore, the $V_{s30}$ for our models (100 m/s for AHA01 and 109 m/s for AHA02) are lower than the $V_{s30}$ values in the NGA database and the GMPE amplification factors are

therefore extrapolated. Nevertheless, we anticipate that the trend of the data should reasonably match the trends in the GMPE amplification factors. Fig. 14 indicates that the slope of the amplification factors from the test data reasonably matches the slope of the amplification factors for the GMPE's. This is an indication that the model test results provide viable results that compare favorably with strong motion records from real earthquakes.

One topic of special interest is the level of base acceleration at which the amplification "saturates," meaning that further decreases of PHA will not lead to increased amplification. As shown in Figure 15, this is set at about 0.05g in the Boore and Atkinson (2008) GMPE. Our results are consistent with this model attribute at 1.0 sec but do not demonstrate clear saturation at short periods.

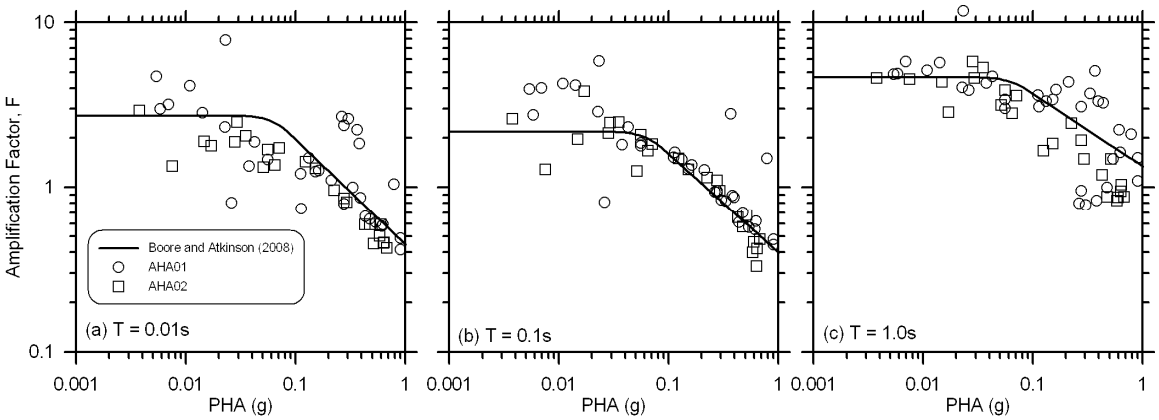


**Figure 15. Amplification factor versus peak horizontal acceleration at (a) T=0.01s, (b) T=0.1, and (c) T=1.0s for all of the ground motions recorded in our research study.**

## 4 CONCLUSIONS

The most fundamental contribution of this research is a publicly available data set for a densely-instrumented soft clay model that was shaken strongly enough to mobilize large shear strains. This data set will be very useful for validating nonlinear site response codes because peak shear

strains of over 1% were mobilized in the clay layers in the centrifuge model. Nonlinear site response codes are widely believed to provide superior results to equivalent linear methods at large strain ($\gamma$>1%), but vertical array recordings corresponding to large shear strain conditions are sparse. The research program utilized a new hinged-plate container at the UC Davis centrifuge that is ideally suited for site response studies because its lateral stiffness is low and it appears to accurately replicate one-dimensional shaking conditions. Previous centrifuge site response studies at UC Davis utilized shear beam containers that can impose undesired boundary conditions on the models. Preliminary analysis of the data demonstrates nonlinear site response effects that are reasonably consistent with empirical nonlinear site amplification factors used in ground motion prediction equations. More research will be required to validate nonlinear site response codes based on the measured test data.

## 5 ACKNOWLEDGMENTS

We would like to thank the NEES@UCDavis personnel, including Dan Wilson, Ross Boulanger, Bruce Kutter, Chad Justice, Ray Gerhard, Peter Rojas, Lars Pederson, Anatoliy Ganchenko, and Jenny Chen for their assistance during this sometimes difficult project. We are also very thankful for the assistance of Brina Mortensen with the bender element coating system and to Ben Mason for calibrating the ground motions utilized in our study. We would like to thank Pat Fox for helping with nonlinear consolidation calculations that helped us understand the process of consolidation from slurry. Steve Dickenson provided some very useful insights about consolidation of fine-grained soils on the centrifuge.

## 6 REFERENCES


Boore, D.M., and Atkinson, G.M. (2008). "Ground-motion prediction equations for the average horizontal component of PGA, PGV, and 5%-damped PSA at spectral periods between 0.01s and 10.0s." *Earthquake Spectra*, 24(1), 99-138.

Elgamal, A., Yang, Z., Lai, T., Kutter, B.L., and Wilson, D.W. (2005). "Dynamic response of saturated dense sand in laminated centrifuge container." *Journal of Geotech. Geoenviron. Eng.*, 131(5). 598-609.

Kramer, S.L. (1996). *Geotechnical Earthquake Engineering*, Prentice Hall, Saddle River, New Jersey. 653 p.

Kramer, S.L. and S.B. Paulsen (2004). "Practical use of geotechnical site response models," *Proc. Int. Workshop on Uncertainties in Nonlinear Soil Properties and their Impact on Modeling Dynamic Soil Response*, PEER Center Headquarters, Richmond, CA

Kwok, AO, JP Stewart, YMA Hashash, N Matasovic, R Pyke, Z Wang, and Z Yang (2007). "Use of exact solutions of wave propagation problems to guide implementation of nonlinear seismic ground response analysis procedures," *J. Geotech. & Geoenv. Engrg.*, ASCE, 133 (11), 1385-1398.

Kwok, AO, JP Stewart, and YMA Hashash, (2008). "Nonlinear ground response analysis of Turkey Flat shallow stiff soil site to strong ground motion," *Bull. Seism. Soc. Am.*, 98(1), 331-343.

Kutter, B. L. (1994): "Recent Advances in Centrifuge Modeling of Seismic Shaking," State-of-the-Art Paper, Proceedings, 3rd International Conference on Recent Advances in Geotechnical Earthquake Engineering and Soil Dynamics, St. Louis, MO, Vol. 2, pp. 927-942, April, 1995.

Ladd, C.C. (1991). "Stability evaluation during staged construction." *J. Geotech. Engrg. Div.*, ASCE, 117(4): 540-615.

Lai, T., Elgamal, A., Wilson, D.W., and Kutter, B.L. (2001). "Numerical modeling for site seismic response in laminated centrifuge container." *Proc. 1st Albert CAQUOT Int. Conf.*, Paris.

Mason, H.B., Kutter, B.L., Bray, J.D., Wilson, D.W., and Choy, B.Y. (2010). "Earthquake motion selection and calibration for use in a geotechnical centrifuge." *7th International Conference on Physical Modeling in Geotechnics*, Zurich Switzerland, July 2010.

Seed, R.B., Dickenson, S.E. and Idriss, I.M. (1991). "Principal geotechnical aspects of the 1989 Loma Prieta earthquake," *Soils and Foundations*, 31 (1), 1-26.